DOI: 10.1007/s12541-011-0146-0

Myoelectric Hand Prosthesis with Novel Adaptive Grasping and Self-locking

Jun-Uk Chu[1], Dong-Hyun Jeong[2], Inchan Youn[1,*], Kuiwon Choi[1,#,*] and Yun-Jung Lee[3]

1 Biomedical Research Institute, Korea Institute of Science and Technology, 39-1, Hawolgok-dong, Seongbuk-gu, Seoul, Korea, 136-791
2 Robotics R&D Group, Daewoo Shipbuilding & Marine Engineering Co. Ltd., 7-1, Dangsan-dong 1-ga, Yeongdeungpo-gu, Seoul, Korea, 150-041
3 School of Electronics Engineering, Kyungpook National University, 1370, Sankyuk-dong, Book-gu, Daegu, Korea, 702-701
Corresponding Author / E-mail: choi@kist.re.kr, TEL: +82-2-958-5921, FAX: +82-2-958-5909
* These authors contributed equally to this paper as corresponding author

KEYWORDS: Hand prosthesis, Underactuation, Adaptive grasping, Self-locking, EMG pattern recognition

This paper presents a novel hand prosthesis controlled by electromyography (EMG) signals. Using an underactuated approach, the hand allows four fingers to flex independently with one actuator, plus the fingers and phalanges provide adaptation with respect to the shape of an object. An innovative self-lock is also embedded in the metacarpophalangeal joint to prevent back-driving when external forces act on the fingers. The thumb is designed to perform flexion/extension and abduction/adduction with one actuator, while the wrist is driven in a differential manner using two actuators. As a result, the hand has eighteen degrees of freedom with only four actuators. Furthermore, it is controlled in real-time by the previously proposed EMG pattern recognition method.[13] Ten kinds of hand motions are classified from four channel EMG signals with a high accuracy and corresponding motion commands are generated for hand control. Experimental results demonstrate the effectiveness of the hand design and validity of the EMG-based hand control.

Manuscript received: April 1, 2011 / Accepted: May 5, 2011

1. Introduction

In recent decades, many myoelectric hands have been developed to imitate the grasping capabilities of the human hand. The first-to-market myoelectric hands, such as the MyoBock hand[1] and ProControl hand,[2] have a good reliability and robustness. However, their mechanism of two rigid fingers and a rigid thumb linked in opposition by a lever and simultaneously actuated by a single motor, is unable to adapt to different object sizes and shapes. More recently, a new myoelectric hand, the i-LIMB hand,[3] became commercially available. This hand allows the four fingers and thumb to stop independently when they come into contact with an object. Yet, the fingers and thumb only provide a fixed curling trajectory and the abduction and adduction of the thumb must be performed manually by the user.

In the field of myoelectric hand design, weight, size, power consumption, and cosmetic appearance are all important factors. However, to improve the grasping capability, a 'fully-actuated' approach requires a large number of actuators for high degrees of freedom. This conflicts with other priorities of myoelectric hand design. Thus, to overcome these limitations, a new design approach, called 'underactuation' has been introduced that can maintain a small number of actuators, while increasing the degrees of freedom. This facilitates 'adaptive grasping', where the fingers and thumb adapt to the shape of a grasped object to increase the contact points between the hand and the object.[4] As a result, underactuated hands can be designed to be light-weight and small in size, while retaining the grasping capabilities of a fully-actuated hand. Until now, a variety of underactuated mechanisms have been proposed, including a compression spring,[4-6] pulley,[6,7] whiffle-tree,[8] adaptive linkage,[9] tendon-routing mechanism,[7,10] and many others.[14]

In particular, the spring mechanism has several advantages over other mechanisms. They are simple and small, and can facilitate adaptive grasping, including shape adaptation between fingers or phalanges. For example, Dechev et al.[4] developed an underactuated hand with a compression spring mechanism that allows the four fingers and thumb to flex inward independently to conform to the shape of an object. Meanwhile, Carrozza et al.[5] proposed a shape adaptation mechanism among fingers and phalanges, where each finger includes cables and compression springs, and each cable is fixed to a corresponding phalanx through each spring. When one link contacts an object, the compression of the corresponding spring allows the other links to continue bending. A linear slider with three pulleys drives all the cables for the fingers, and three pairs of cables

for the index and middle fingers are wrapped around the respective pulleys to provide shape adaptation among the fingers. However, the main drawback is that spring compression requires a linear transmission system, such as a slider, lead screw, and ball nut, which causes the overall system to be bulky and complex. In addition, when the spring is not fully compressed by the slider to an intermediate position, the fingers can be back-driven by external forces.

In order to rectify these undesirable features, a novel design method is proposed using a spiral spring and cam-roller mechanism. The winding of the spiral spring provides shape adaptation between the fingers in the restricted volume of the metacarpophalangeal joint and an embedded cam-roller mechanism guarantees the self-locking of each finger. Based on this mechanism, a multifunction myoelectric hand is presented which is composed of four pairs of spiral springs, cams, and rollers; four fingers capable of adaptation between the phalanges; a thumb with the movements of flexion/extension and abduction/adduction; and a wrist allowing six motions, such as flexion/extension, radial/ulnar flexion, and pronation/supination. This paper describes the detail design of the proposed hand, and evaluates the mechanical performance including adaptive grasping and self-locking function. In addition, the hand is applied to normal subjects for the purpose of demonstrating the feasibility of the EMG pattern recognition for real-time motion control.

2. Hand Design

The hand is a five-fingered hand with a wrist, as shown in Fig. 1. The design concept includes five functional features:

1) The hand allows the fingers and thumb to flex independently to increase the contact points between the hand and an object.
2) Each finger and thumb has a self-locking function against external forces.
3) For each finger and thumb, the three phalanges can flex independently to wrap an object with multi-point contact.
4) The thumb performs abduction/adduction.
5) The wrist allows pronation/supination, radial/ulnar flexion, and flexion/extension.

Meanwhile, the design constraints are as follows:

1) For the fingers and thumb, the number of motors is limited to only two and they are placed in the palm.
2) For the wrist, the number of motors is limited to only two and they are placed in the forearm.

To realize the above features within the constraints, five novel mechanisms are proposed, as described in detail in the following subsections.

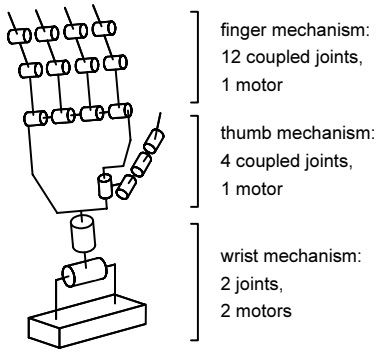

Fig. 1 Design concept and constraints

2.1 Metacarpophalangeal Joint Design

An underactuated mechanism using a spiral spring is proposed to allow for relative displacement of the fingers when an irregular object is grasped. Figure 2 presents a simplified schematic of this mechanism. In the metacarpophalangeal joints, each spiral spring is wound around and fixed to a shaft, which is actuated by one motor. Each finger is combined with a corresponding spiral spring through a housing. The springs are surrounded by the housing in order to reduce the space needed and maintain the deflection. Then, the housing is supported by a holder allowing free-wheeling motion possible.

When the hand grasps an irregular object, shape adaptation between fingers is obtained by the operation of the spiral springs. As shown in Fig. 3, there are four states in this operation according to the grasping mode: reaching, adaptation, power grasp, and release mode. The reaching mode begins from the fully extended motion of the finger, and closes at the instant of an object's contact (Fig. 3(a)). In this mode, the spiral spring, having a small amount of

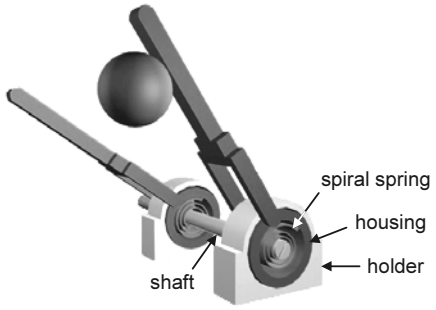

Fig. 2 Spiral spring mechanism for shape adaptation between fingers

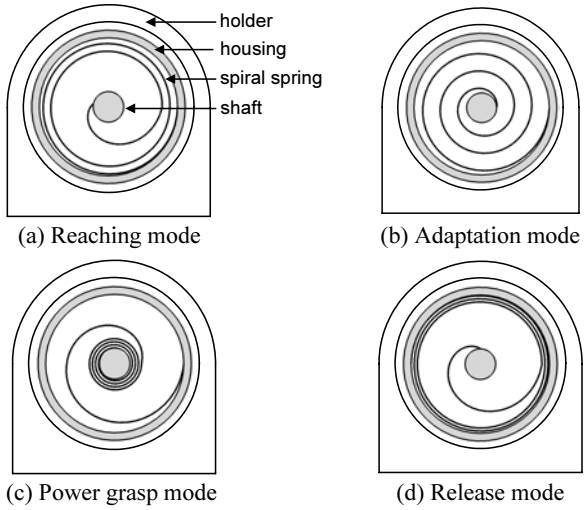

Fig. 3 Four operating states of spiral spring mechanism

deflection, transmits the motor's power to the finger directly. In the adaptation mode (Fig. 3(b)), when one finger maintains contact with an object, the spiral spring is wound up and stores the motor's power. This operation enables the other non-contact fingers to keep flexion motion. Each finger has a grasping force proportional to the winding of the corresponding spiral spring. During the power grasp mode (Fig. 3(c)), the spiral spring is fully wound up to the shaft so that the spiral spring and housing operate as a rigid wheel attachment between the shaft and finger. The grasping force directly depends on the motor's rotation. In the release mode (Fig. 3(d)), the finger is removed from the object and returns to the initial extended position. The reverse rotation of the motor causes the spiral spring to be unwound back to the inside of the housing, in contrast to the power grasp mode.

Despite the advantages of the proposed spiral spring design, there are two shortcomings that need to be addressed. Firstly, the spring can be deflected by external forces that arise when the user moves their wrist or arm, or when an object's weight varies. And secondly, a continuous motor torque should be applied to the fingers for sustaining a grasp. Commercially available myoelectric hands usually provide a self-lock element. This is located between the motor and the gear box to prevent rigid fingers from back-driving and conserves the battery's power.[1,2] However, this method is only feasible under limited conditions when all fingers are simultaneously driven by one motor. Therefore, a self-lock element for each finger is proposed, which can be equipped in each metacarpophalangeal joint. The self-lock element of this design allows unidirectional power transmission from the driving part to the driven part, and uses the principle of a conventional cam-roller clutch. To give a better explanation of this mechanism, a schematic of the proposed self-lock is shown in Fig. 4. The self-lock is composed of a driving plate, driven plate, holder, and rollers. The driving plate has cam surfaces with the same curvature as the opposite side of the holder. The distance between the cam surface and the opposite side of the holder is larger than the roller's diameter. Therefore, in any rotating direction, the driving plate can always carry the rollers without friction force. In the driven plate, inclined cam surfaces are arranged symmetrically with respect to the horizontal and vertical axes. The contact between the inside of the holder and the driven plate's inclined cam surfaces imparts a friction force to the rollers. As a result, one pair of rollers is tightly wedged together whenever the driven plate is arbitrarily rotated by external forces, prohibiting back-driven motions.

The operation of the cam-roller is divided into four states in accordance with driving/locking function and clockwise/counter-clockwise direction. Figure 5 illustrates how to attain unidirectional power transmission during the operating states of the cam-roller. The solid and dashed lines indicate the driven and driving plates, respectively. The solid and dashed arrows around the shaft denote the direction of each plate's rotation. When the driving plate rotates counter-clockwise (Fig. 5(a)), rollers 2 and 4 lie between the edges of the two cam surfaces of the driven plate and driving plate and connect the two plates to transfer rotary power. Meanwhile, rollers 1 and 3 are in a free-wheeling mode and have no influence on the rotation. As a result, this configuration prevents all of the rollers from wedging and allows rotation with no friction. In the reverse configuration (Fig. 5(b)), the rollers are engaged in clockwise driving and their modes are changed from free-wheeling, rollers 1 and 3, to connecting or from connecting, rollers 2 and 4, to free-wheeling. During the counter-clockwise self-locking (Fig. 5(c)), when an external torque is applied to the driven plate, rollers 2 and 4 are wedged between the inclined cam surface and the inside of the holder. Rollers 1 and 3 are not involved in the locking motion. This mechanism is based on the same principle as a one-way clutch. In the reverse direction (Fig. 5(d)), clockwise self-locking is conducted by the rollers 1 and 3, whose modes are switched from free-wheeling to wedging.

A detailed view of the metacarpophalangeal joint is shown in Fig. 6. On the basis of the spiral spring and cam-roller mechanism, a metacarpophalangeal joint design is proposed to incorporate

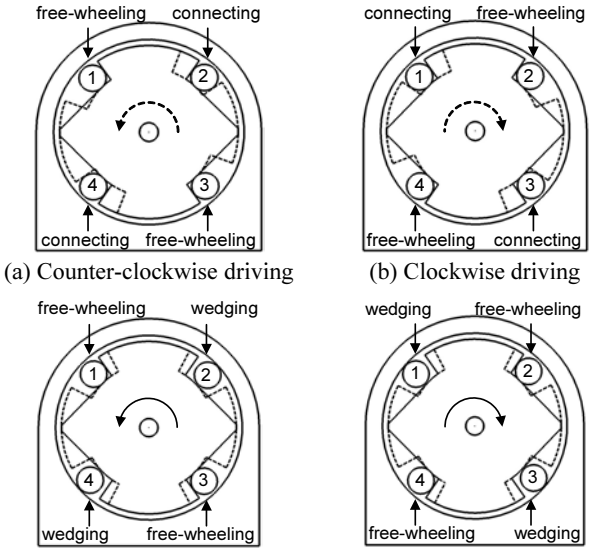

Fig. 5 Four operating states of cam-roller mechanism

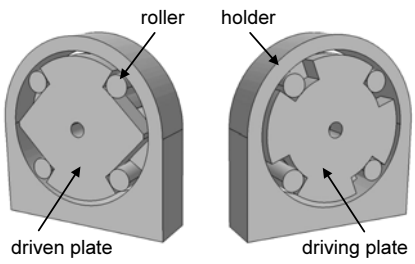

Fig. 4 Cam-roller mechanism for self-locking

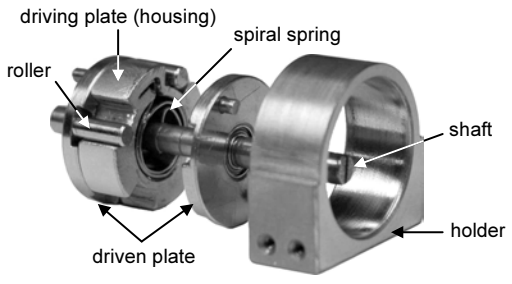

Fig. 6 Metacarpophalangeal joint module

adaptive grasping and self-locking function. To realize these functions in the constrained joint space, the spiral spring's housing is designed to have the same cam surfaces as the self-locking element's driving plate. The spiral spring is also enclosed by the housing and wound around the shaft. The driven plate is attached to the shaft through a bearing and has two hinge pins to connect each finger. Furthermore, two driven plates are located on both sides of the housing to improve the power transmission reliability and connectivity of the finger mechanism. Finally, all the above elements are supported by the holder to enable free-wheeling motion. Therefore, four rollers are engaged with the inside of the holder, the inclined cam surfaces of the two driven plate, and the concentric circular cam surfaces of the driving plate.

2.2 Finger Design

An underactuated finger is proposed based on a seven-bar mechanism to facilitate adaptive grasping between phalanges. Figure 7 presents a side section view of the finger module assembled with a metacarpophalangeal joint. From the original seven-bar mechanism,[11] the proximal four-bar mechanism is modified to connect the proximal phalanx to the metacarpophalangeal joint. That is, the input link of the four-bar mechanism is replaced by the driven plate with hinge pins. The middle four-bar mechanism is coupled with the proximal one through a triangular link to provide shape adaptation for the proximal interphalangeal joint. Furthermore, the distal interphalangeal joint is designed to attach the distal phalanx to the output link of the middle four-bar mechanism.

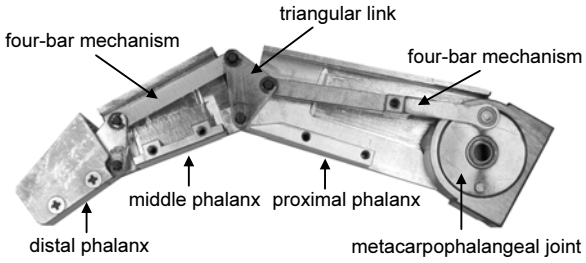

Fig. 7 Finger module

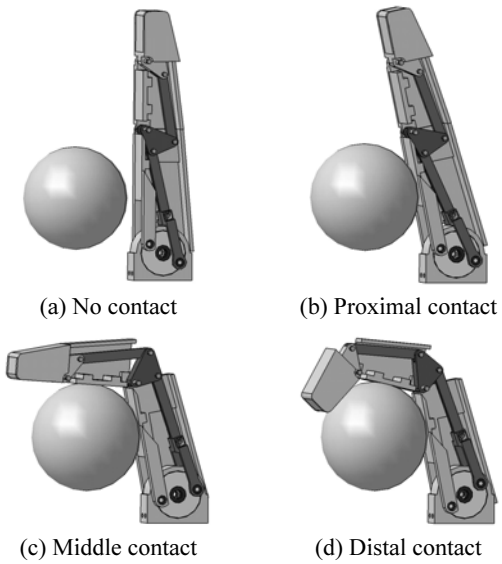

(a) No contact (b) Proximal contact

(c) Middle contact (d) Distal contact

Fig. 8 Sequential contact of phalanges

Figure 8 shows how to achieve shape adaptation between phalanges while the finger is flexed. The three phalanges behave as one rigid link before the finger encounters an object (Fig. 8(a)). However, once the proximal phalanx contacts the object, the middle phalanx begins to flex (Fig. 8(b)). Then, when the middle phalanx meets the object, and the distal phalanx begins to flex (Fig. 8(c)). Eventually, the object is wrapped by the three phalanges with multi-point contact (Fig. 8(d)).

2.3 Thumb Design

The thumb can perform adaptive grasping using the modified seven-bar mechanism like the fingers. In addition, it has abduction and adduction function in the carpometacarpal joint, which are implemented by an intermittent mechanism. As an example of similar approaches, the Manus hand[12] used a timing gear to provide cyclic movement. However, in that hand design, the movement of the carpometacarpal joint was coupled with that of the interphalangeal joint, and the motor's power was transmitted by a complex driven path. In order to improve the efficacy of using an intermittent mechanism, an external Geneva wheel and crank-slider mechanism is adopted in the design of thumb. The complete

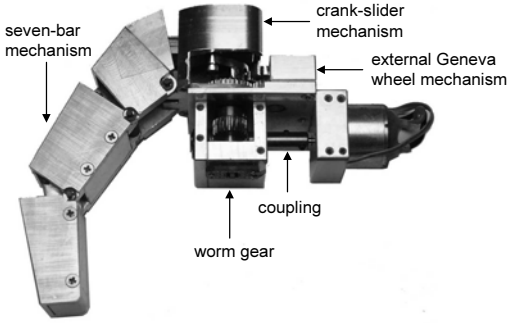

Fig. 9 Thumb module

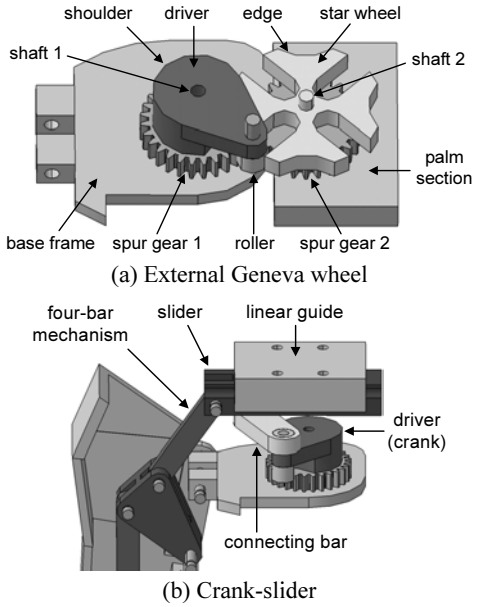

(a) External Geneva wheel

(b) Crank-slider

Fig. 10 Schematic diagram of thumb mechanism

assembly of thumb module is shown in Fig. 9. Four degrees of freedom are actuated with only one single motor through a worm gear, which also provides self-locking for all the joints.

The external Geneva wheel mechanism is composed of a star wheel, roller, driver, and spur gear set (Fig. 10(a)). Spur gear 1 is connected with the thumb's base frame and attached to shaft 1 through a bearing. However, the driver is not connected to the thumb's base frame but fixed to shaft 1. Spur gear 2 and the star wheel are welded into one body and attached to shaft 2 of the palm section through a bearing. As a result, the thumb's base frame can only be rotated when the spur gear set transmits rotational movement. In the crank-slider mechanism, the external Geneva wheel's driver is used as a crank and coupled with the slider through a connecting bar (Fig. 10(b)). The thumb has three phalanges and the design is similar to that of the fingers. To generate flexion and extension, the end of the proximal four-bar mechanism is connected to the slider and thumb's base frame.

Figure 11 shows the cyclic movement of the thumb according to the shaft angle. The cycle starts from the maximally flexed position of a cylindrical grasp (Fig. 11(a)). By virtue of the crank-slider mechanism, the intermittent rotary motion is changed to a reciprocating linear motion. During the clockwise rotation of the shaft, the slider is pulled so that the thumb is opened (Fig. 11(b)). Eventually the phalanges are completely extended (Fig. 11(c)). The roller is at the point of entering the slot and begins to drive the star wheel (Fig. 11(d)). A spur gear set is used to transfer the intermittent rotary motion to the thumb's base frame for abduction and adduction (Fig. 11(e)). The star wheel is locked during its rest periods, as the concentric shoulder of the driver has engaged the corresponding edge of the star. As a result, abduction and adduction are only possible when the phalanges are completely extended. The star wheel motion then ceases when the roller has moved through a $\pi/2$ angle (Fig. 11(f)). If the shaft continues to rotate in the same direction, the slider is pushed for the thumb to perform flexion of the lateral grasp (Figs. 11(g)-(h)).

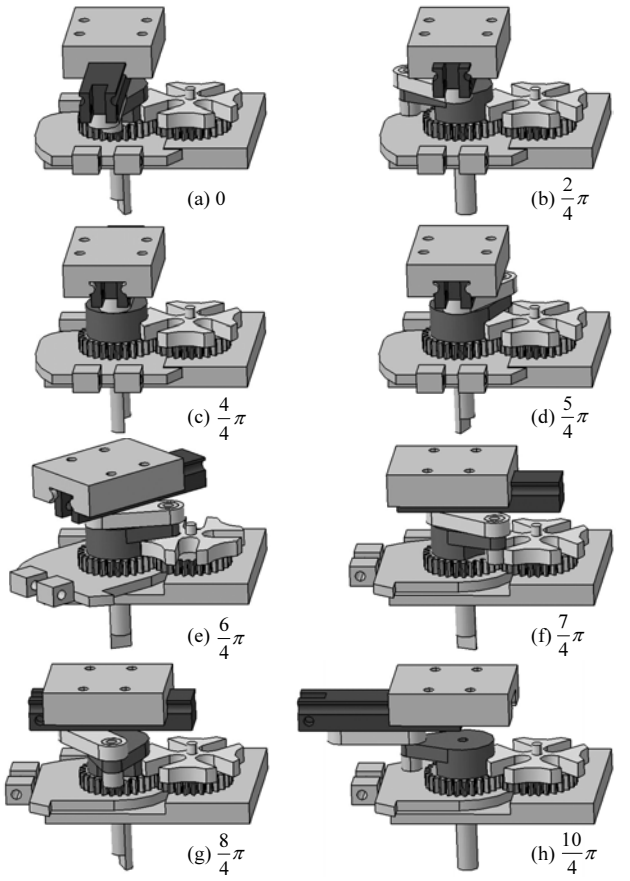

Fig. 11 Cyclic movement of thumb mechanism according to shaft angle

2.4 Palm and Wrist Design

Figure 12 shows a palmar view of the proposed hand, except for the palm section. As mentioned previously, the number of motors for the fingers and thumb is limited to only two and they are placed in the palm. While one motor drives the four fingers with a 29:1 planetary gear, spiral spring, and cam-roller mechanism, the other actuates the thumb through a 20:1 worm gear, external Geneva wheel, and crank-slider mechanism. When the hand adaptively grasps an object, the spiral spring is wound around the shaft. To allow the hand to maintain the grasping force, the fingers' motor should supply rotary power to the shaft continuously. However, using the proposed cam-roller mechanism, another self-lock is embedded in the motor and connected to the shaft through the spur gear. As a result, the spiral spring remains in a wound state without continuous motor driving.

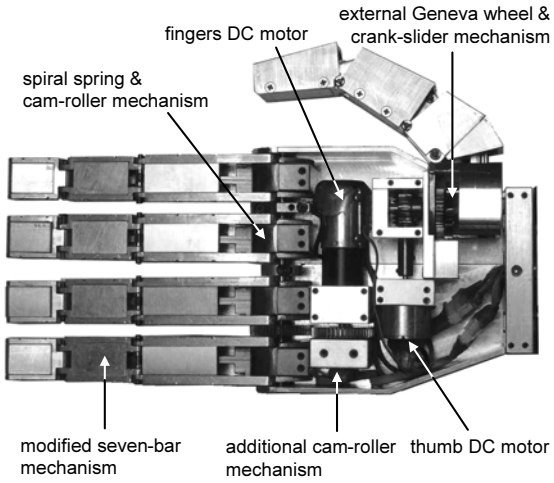

Fig. 12 Palm structure

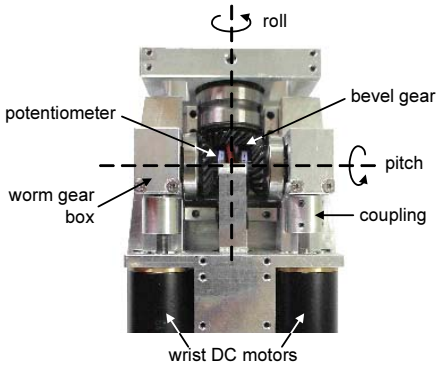

Fig. 13 Wrist module

Wrist motion plays an important role for the hand to naturally and easily approach an object. Therefore, the wrist module of the prosthetic hand is actuated in a differential manner through two DC motors. The actuation system consists of three bevel gears and two worm gear sets, as shown in Fig. 13. This configuration has two degrees of freedom and allows a roll and pitch motion using the power of the two motors. According to the combination of the two motors' rotation, the wrist can perform flexion/extension, radial/ulnar flexion, and pronation/supination. Although flexion/extension and radial/ulnar flexion are possible depending on the roll position, these motions are useful when picking up an object that is higher than the level of the elbow or when using a knife to chop up food.

3. Results

3.1 Prototype Hand Prosthesis

A prototype of the proposed hand was made according to the design concepts described above (Fig. 14). Its specifications are presented in Table 1. The hand is almost the same size as a male adult's hand and slightly heavier than other commercially available hands. In addition, the hand's appearance is similar to that of a human hand. The frames were all made of light-weight aluminum, while the self-lock element and gear set were constructed using stainless steel for abrasion resistance. Although it only uses four DC motors, the hand has 18 degrees of freedom. The hand motions are controlled by a digital signal processor (DSP) and pair of motor driver circuits. For position feedback, four small and flat potentiometers are attached to the shafts and wired to an analog-to-digital converter (ADC) embedded in the DSP. Based on its mechanical design features and control system, the hand can perform versatile grasp and wrist motions. These motion commands are generated by an EMG pattern recognizer and sent to the hand motion controller via a serial communication interface (SCI).

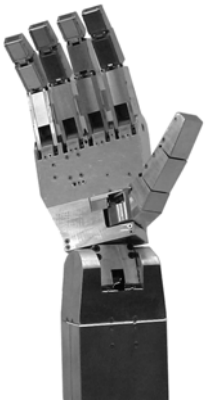

Fig. 14 Prototype hand prosthesis

Table 1 Specifications of Hand

Components	Specifications	
	Hand	Wrist
Dimensions (mm)	190L x 90W x 30H	100L x 70W x 40H
Weight (g)	800	200
Degrees of freedom	16	2
Actuators	Two DC motors	Two DC motors
Sensors	Two potentiometers	Two potentiometers
Controller	TMS320F2812	
Materials	Aluminum and stainless steel	

3.2 Grasping Performance

In this experiment, the hand was operated using the hand motion controller without an EMG pattern recognizer. The motion commands were generated using push button switches and sent to the hand motion controller via a digital input port. The command set consisted of 'OPEN', 'CYLINDRICAL', and 'LATERAL'. Although a cylindrical and tip grasp use the same motion command 'CYLINDRICAL', and a hook and lateral grasp use the same motion command 'LATERAL', the grasping motions were automatically changed according to the shape of the object. Therefore, the adaptive grasping capability of the proposed prosthetic hand means that only two commands, instead of four, are needed for cylindrical, tip, hook, and lateral grasping motions.

Figure 15 shows that the hand prosthesis performed four grasping motions and was capable of adaptively grasping variously shaped objects. The spiral spring and modified seven-bar mechanism allowed shape adaptation between the fingers and between phalanges, respectively. The external Geneva wheel and crank-slider mechanism also created good thumb motion, including flexion, extension, abduction, and adduction.

3.3 Self-locking Performance

An experiment was also performed to test the self-locking of the proposed cam-roller mechanism. As a means of quantifying the

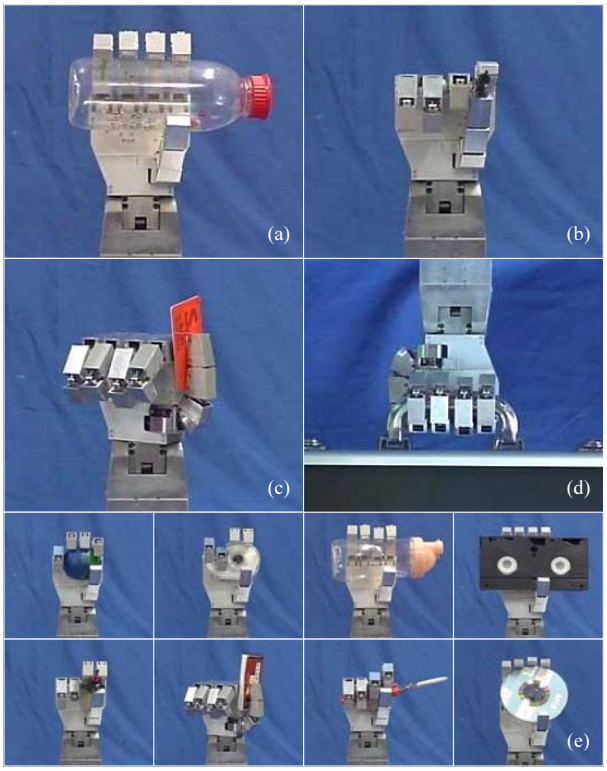

Fig. 15 Grasping motions of proposed hand: (a) cylindrical grasp, (b) tip grasp, (c) lateral grasp, (d) hook grasp, and (e) other adaptive grasps

self-locking performance, the grasping force was measured at the finger tips. In the experimental setup the hand performed a tip grasp, and a digital push-pull force gauge was used to measure the grasping force. Two steel plates were mounted on both the test bench and the gauge to provide the fingers with a contact area to apply force. The distance between the plates was set to 20, 40, and 60 mm. The configuration of the joints was automatically determined by the adaptive grasping of the fingers and thumb. Figure 16 shows the force response during the tip grasping. After the force reached a predetermined value for each grip distance, the power source of the motors was disconnected. Nonetheless, the hand maintained its grasping force for any grip distance due to the self-locking capability of the cam-roller mechanism. The arrowhead indicates the instant when the motors turned off.

3.4 EMG-based Hand Control Performance

In previous research,[13] a learning method for Gaussian mixture models (GMMs) was proposed to improve their EMG pattern recognition accuracy. The proposed learning method provided stable parameter and model order estimates using the conjugate priors of the GMM. The parameters were estimated using a maximum a posterior (MAP)-based expectation-maximization (EM) algorithm in which the conjugate priors prevented a singular solution. In the model order selection criterion, the conjugate priors penalized a model for which the parameter estimate was overfitted. The proposed conjugate-prior-penalized learning method resulted in a superior generalization performance when compared to other learning methods. Plus, when using the proposed GMM classifier, ten kinds of motion were recognized from four EMG channels with a high recognition accuracy.

This method especially produced good classification results for analogous motions, such as a cylindrical and tip grasp or hook and lateral grasp. However, these motions generate similar EMG patterns. This causes different class features to overlap in the feature space, thereby forcing the user to concentrate on hand control to prevent the generation of undesired motions. This problem can be solved by the adaptive grasping capabilities of the proposed hand. As shown in the grasping performance test, the hand automatically changed the grasping motions according to the shape of the object, and performed four grasping motions using just two commands. Consequently, analogous EMG patterns, such as a cylindrical and tip grasp or hook and lateral grasp can be classified as one motion, allowing the user to operate the hand naturally without any additional attention.

Accordingly, an experiment was performed to simultaneously demonstrate the effectiveness of the hand design and the validity of the EMG-based hand control. The GMM-based EMG pattern recognizer was configured to classify ten kinds of hand motions: flexion (F) and extension (E) of the wrist, radial flexion (RF) and ulnar flexion (UF) of the wrist, pronation (P) and supination (S) of the wrist, opening (O), cylindrical (C) and lateral (L) grasping of

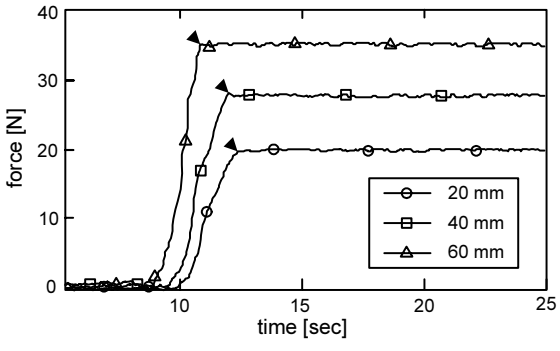

Fig. 16 Grasping force during self-locking performance test

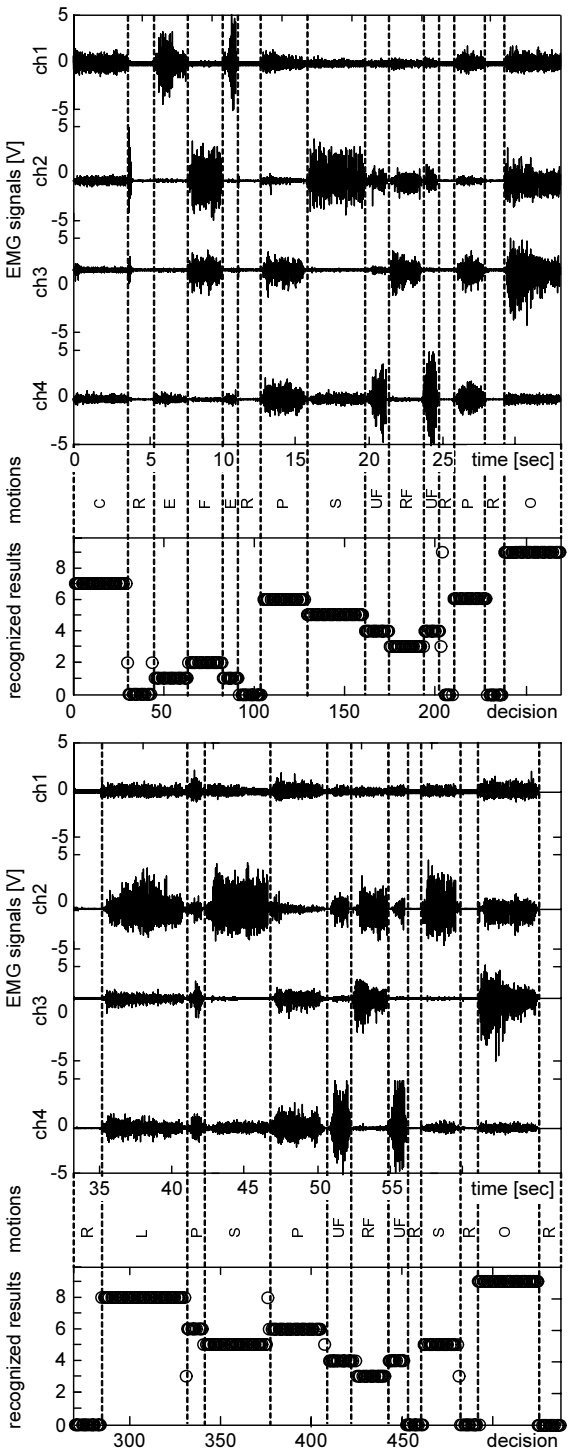

Fig. 17 EMG signals and recognized results in real-time experiment

the fingers and thumb, and relaxation (R). Four surface electrodes were used to measure the EMG signals from the extensor digitorum, extensor carpi radialis, palmaris longus, and flexor carpi ulnaris. In the learning procedure, the parameters and model order for GMM classifier were specified with respect to the subject and hand motion. After determining the parameters and model orders, the proposed method was used to implement a real-time EMG pattern recognition system for the hand control. The recognition program was developed on a 2.4 GHz Pentium IV personal computer (PC). The experimental setup included four surface electrodes, a filter-and-amplifier module, PC with ADC board and SCI port, graphic user interface, DSP motion controller, and the prototype hand. For real-time implementation, all the processing, such as the segmentation, feature extraction, GMM classification, and communication with the motion controller, was performed within the window increment (125 msec) for every decision. During the testing of the hand control, the graphic user interface displayed information about the four-channel EMG signals, the results of the EMG pattern classification, and the graphic hand.

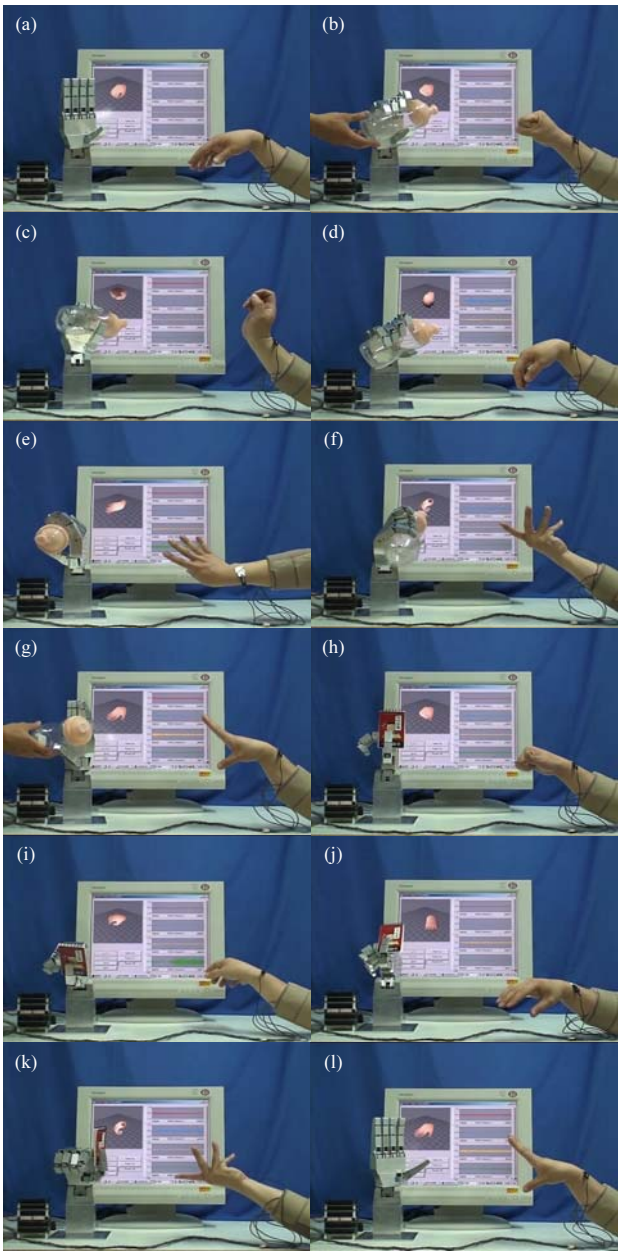

Fig. 18 Real-time EMG pattern recognition for hand control: (a) relaxation, (b) cylindrical grasp, (c) extension, (d) flexion, (e) pronation, (f) supination, (g) open, (h) lateral grasp, (i) ulnar flexion, (j) radial flexion, (k) supination, and (l) open

Figure 17 shows the four-channel EMG signals and recognized results when the normal subject operated the hand. The separated motion labels just indicate the change of the hand motion with time, rather than the accurate time interval occupied by each motion. For the recognized results, each motion was assigned a number from 0 to 9, and an open circle used to denote the recognized motion. Several incorrect classifications occurred at the beginning and ending of the motions and caused small errors in the hand motion. However, these errors were promptly suppressed by subsequent correct classifications and the operator did not perceive any errors while controlling the hand. Figure 18 shows the proposed hand controlled by the EMG pattern recognition results. In Figs. 18(a)-(g), the hand grasped an irregular cylindrical object, executed some wrist functions, and then released the object. Also, a lateral grasping motion was performed on a notepad, as shown in Figs. 18(h)-(l). Therefore, these results confirm that the proposed prosthetic hand can be controlled by the GMM-based EMG pattern recognition method.

4. Conclusion

This paper proposed a new myoelectric hand system for upper-limb deficient individuals. The hand system is composed of a mechanical hand and EMG pattern recognizer. To improve the grasping capabilities, novel underactuated designs were proposed that include spiral spring, cam-roller, modified seven-bar, external Geneva wheel, crank-slider, and bevel gear differential mechanism. As a result, the hand can perform versatile grasp and wrist motions using only four motors. It is capable of natural and stable grasping without complex servo and sensor systems. Moreover, the adaptive grasping capabilities reduce the requirements of EMG pattern recognition, since analogous motions, such as a cylindrical and tip grasp or lateral and hook grasp, can be classified as one motion. The EMG pattern recognition is constructed based on a Gaussian mixture model, and the GMM classifier can discriminate hand motions with a high accuracy, allowing it to be used to implement real-time EMG pattern recognition for hand prosthesis control.

ACKNOWLEDGEMENT

This research was partially supported by the Pioneer Research Center Program through the National Research Foundation of Korea funded by the Ministry of Education, Science and Technology (20100019348), the Public welfare & Safety research program through the National Research Foundation of Korea (NRF) funded by the Ministry of Education, Science and Technology (20100020786), and Priority Research Centers Program through the

National Research Foundation of Korea (NRF) funded by the Ministry of Education, Science and Technology (2010-0020089).

REFERENCES

1. Motion Control Inc., "ProControl Hand," http://www.utaharm.com, 1987.
2. Otto Bock Healthcare, "MyoBock Hand," http://www.ottobock.com, 1987.
3. Touch EMAS Ltd., "i-LIMB Hand," http://www.touchbionics.com, 2007.
4. Dechev, N., Cleghorn, W. L. and Naumann, S., "Multiple Finger, Passive Adaptive Grasp Prosthetic Hand," Mechanism and Machine Theory, Vol. 36, No. 10, pp. 1157-1173, 2001.
5. Carrozza, M. C., Suppo, C., Sebastiani, F., Massa, B., Vecchi, F., Lazzarini, R., Cutkosky, M. R. and Dario, P., "The SPRING Hand: Development of a Self-Adaptive Prosthesis for Restoring Natural Grasping," Autonomous Robots, Vol. 16, No. 2, pp. 125-141, 2004.
6. Massa, B., Roccella, S., Carrozza, M. C. and Dario, P., "Design and Development of an Underactuated Prosthetic Hand," Proc. of the IEEE Int. Conf. Robotics and Automation, Vol. 4, pp. 3374-3379, 2002.
7. Dollar, A. M. and Howe, R. D., "The SDM Hand as a Prosthetic Terminal Device: A Feasibility Study," Proc. of the IEEE 10th Int. Conf. Rehabilitation Robotics, pp. 978-983, 2007.
8. Kyberd, P. J., Light, C., Chappell, P. H., Nightingale, J. M., Whatley, D. and Evans, M., "The Design of Anthropomorphic Prosthetic Hands: A Study of the Southampton Hand," Robotica, Vol. 19, No. 6, pp. 593-600, 2001.
9. Zhao, J., Jiang, L., Shi, S., Cai, H., Liu, H. and Hirzinger, G., "A Five-fingered Underactuated Prosthetic Hand System," Proc. of the IEEE Int. Conf. Mechatronics and Automation, pp. 1453-1458, 2006.
10. Carrozza, M. C., Cappiello, G., Micera, S., Edin, B. B., Beccai, L. and Cipriani, C., "Design of a Cybernetic Hand for Perception and Action," Biological Cybernetics, Vol. 95, No. 6, pp. 629-644, 2006.
11. Laliberte, T. and Gosselin, C. M., "Underactuation in Space Robotic Hands," Proc. of the 6th Int. Symp. Artificial Intelligence, Robotics & Automation in Space, 2001.
12. Pons, J. L., Rocon, E., Ceres, R., Reynaerts, D., Saro, B., Levin, S. and Van Moorleghem, W., "The MANUS-HAND Dextrous Robotics Upper Limb Prosthesis: Mechanical and Manipulation Aspects," Autonomous Robots, Vol. 16, No. 2, pp. 143-163, 2004.
13. Chu, J. U. and Lee, Y. J., "Conjugate-Prior-Penalized Learning of Gaussian Mixture Models for Multifunction Myoelectric Hand Control," IEEE Trans. Neural Systems and Rehabilitation Engineering, Vol. 17, No. 3, pp. 287-297, 2009.
14. Kim, E. H., Lee, S. W. and Lee, Y. K., "A Dexterous Robot Hand with a Bio-mimetic Mechanism," Int. J. Precis. Eng. Manuf., Vol. 12, No. 2, pp. 227-235, 2011.